

## Supplementary material for:

### From açaí (*Euterpe oleracea* Mart.) waste to mannose and mannanoligosaccharides: a one-step process for recalcitrant mannan depolymerization using dilute oxalic acid

Fernanda Thimoteo Azevedo Jorge<sup>1</sup>, Ingrid Santos Miguez<sup>1,2</sup>, George Victor Brigagão<sup>3</sup>,  
Ayla Sant'Ana da Silva<sup>1,2\*</sup>

<sup>1</sup> Laboratório de Biocatálise, Instituto Nacional de Tecnologia, Ministério da Ciência, Tecnologia e Inovações, Rio de Janeiro, 20081-312, RJ, Brazil

<sup>2</sup> Departamento de Bioquímica, Universidade Federal do Rio de Janeiro, Rio de Janeiro, 21941-909, RJ, Brazil

<sup>3</sup> Departamento de Engenharia Industrial, Escola Politécnica, Universidade Federal do Rio de Janeiro, Rio de Janeiro, 21941-909, RJ, Brazil

\*Corresponding author: [ayla.santana@int.gov.br](mailto:ayla.santana@int.gov.br)

## Table of contents

Table S1. Açaí seeds chemical composition .....	2
Table S2. Premises and parameters for the biomass handling process section (S-100).....	2
Table S3. Operational parameters for the polyphenols extraction process section (S-200).....	3
Table S4. Operational parameters for the acid hydrolysis process section (S-300).....	4
Table S5. Operational parameters for the mannose purification section (S-500) .....	5
Table S6. Operational parameters for the MOS purification section (S-600).....	6
Table S7. Operational parameters for the combustion section (S-700) .....	6
Table S8. Operational parameters for the cold utilities section (S-800) .....	7
Table S9. Analysis of variance of the adjusted models for mannose yield, mannan conversion, and mass loss for oxalic acid hydrolysis of açaí seeds.....	8
Figure S1. Theoretical and experimental pH values of oxalic acid solutions at different concentrations and experimental pH values of açaí seeds hydrolysates after dilute oxalic acid hydrolysis. Theoretical pH values for sulfuric acid solutions are also shown for comparison.....	10
Figure S2. Correlations between the combined severity factor and response variables of dilute-oxalic acid hydrolysis of açaí seeds optimization: a) mannose yield, b) mannan conversion, c) mass loss.....	11

## 1. Parameters for techno-economic analysis

Table S1. Açaí seeds chemical composition

<b>Component</b>	<b>Ref<sup>1</sup></b>	<b>Ref<sup>2</sup> - lot 1</b>	<b>Ref<sup>2</sup> - lot 2</b>	<b>This study</b>	<b>Average</b>	<b>Normalized average<sup>a</sup></b>
Mannan	48.24%	47.09%	52.46%	50.55%	49.58%	53.89%
ARS <sup>b</sup>	17.30%	18.34%	19.54%	20.85%	19.01%	20.66%
Extractives	9.50%	15.45%	9.89%	11.81%	11.66%	12.68%
Glucan	7.79%	6.09%	8.40%	5.77%	7.01%	7.62%
Xylan	2.80%	1.83%	2.05%	1.84%	2.13%	2.32%
Galactan	1.29%	1.79%	1.51%	1.31%	1.47%	1.60%
Ashes	0.16%	0.61%	0.44%	1.56%	0.69%	0.75%
Arabinan	0.61%	0.40%	0.63%	0.00%	0.41%	0.44%
<b>Sum</b>	<b>87.7%</b>	<b>91.6%</b>	<b>94.9%</b>	<b>93.7%</b>	<b>92.0%</b>	<b>100.0%</b>

<sup>a</sup> Values used for process simulations

<sup>b</sup> Acid resistant solids, modelled as lignin

Table S2. Premises and parameters for the biomass handling process section (S-100)

<b>Equipment and parameters</b>	<b>Values</b>
<b>Storage silo</b>	
Biomass bulk density (kg/m <sup>3</sup> )	738 <sup>3,4</sup>
Storage time (days)	1
<b>Rotary Dryer</b>	
Incoming moisture content	45% <sup>5</sup>
Final moisture content	10%
Drying capacity (kg/m <sup>2</sup> h)	30 <sup>6</sup>
<b>Mill and storage silo</b>	
Mill energy consumption (kWh/t)	21 <sup>7</sup>
Milled biomass density (kg/m <sup>3</sup> )	518
Storage time (days)	3

Table S3. Operational parameters for the polyphenols extraction process section (S-200)

<b>Equipment and parameters</b>	<b>Values</b>
<b>Extractor</b>	
Total solids (%wt)	14%
Ethanol concentration (%wt)	50%
Temperature (°C)	60
Residence time (min)	30
Extraction efficiency	95%
<b>Desolventizer</b>	
Ethanol recovery	99.99%
Inlet vapor temperature (°C)	125
<b>Multi-effect Evaporator</b>	
Temperature (°C)	85 / 75 / 60
Pressure (atm)	1.061 / 0.557 / 0.201
Heat transfer coefficients (kW/m <sup>2</sup> °C)	2.98 / 2.56 / 1.85
<b>Spray dryer</b>	
Final moisture content	4%
Product recovery	90%

Table S4. Operational parameters for the acid hydrolysis process section (S-300)

Equipment and parameters	Alternatives 1&1B	Alternative 2
<b>Vertical impregnation tank <sup>a</sup></b>		
Total solids (wt%) <sup>8</sup>	40%	40%
Acid concentration (wt%)	6.0%	4.0%
Temperature (°C)	177	153
Pressure (atm)	8.95	4.95
Residence time (min) <sup>8</sup>	10	10
<b>Horizontal reactor <sup>a</sup></b>		
<b>Operating conditions</b>		
Total solids (wt%) <sup>8</sup>	30%	30%
Acid concentration (wt%)	6.0%	4.0%
Temperature (°C)	177	150
Pressure (atm)	8.73	5
Residence time (min)	15	65.2
Combined severity factor	2.47	2.24
<b>Reactions and conversions</b>		
(Mannan) <sub>n</sub> + n H <sub>2</sub> O → n Mannose	82.56%	57.80%
(Glucan) <sub>n</sub> + n H <sub>2</sub> O → n Glucose	44.33%	57.80%
(Xylan) <sub>n</sub> + n H <sub>2</sub> O → n Xylose	82.09%	65.96%
(Galactan) <sub>n</sub> + n H <sub>2</sub> O → n Galactose	86.90%	100.00%
(Lignin) <sub>n</sub> → n Soluble Lignin	23.62%	11.36%
Hexoses → HMF + 3H <sub>2</sub> O	1.90%	0.80%
Pentoses → Furfural + 3H <sub>2</sub> O	35.70%	34.04%
<b>Blowdown tank</b>		
Pressure (atm)	1.00	
Temperature (°C)	102	
Residence time (min)	15	
<b>SMB chromatography</b>		
Desorbent/feed ratio (v/v)	2 <sup>9-11</sup>	
Oxalic acid recovery in the raffinate	97% <sup>10,12</sup>	
Sugars recovery in the eluate	95% <sup>10,12</sup>	

<sup>a</sup> The reactor design includes a vertical presteamer vessel, two transport conveyors, and two plug screw feeders to the horizontal screw reactor, according to a reactor design by Humbird et al.<sup>8</sup> The continuous screw reactor is sized considering the hydrolysis reaction time and a 40% filling degree<sup>13</sup>.

Table S5. Operational parameters for the mannose purification section (S-500)

<b>Equipment and parameters</b>	<b>Values</b>
<b>SMB Chromatography</b>	
<b>Stream</b>	<b>Flow ratio <sup>14</sup></b>
Feed	1.0
Eluent (deionized water)	3.9
Extract (mannose rich stream)	2.9
Raffinate (other sugars)	2.0
<b>Component</b>	<b>Split fraction in the extract <sup>14</sup></b>
Arabinose	1.000
Mannose	0.949
Xylose	0.216
Galactose	0.103
Glucose	0.063
MOS <sup>a</sup>	0.003
<b>Multi-effect Evaporator</b>	
	1 <sup>st</sup> / 2 <sup>nd</sup> / 3 <sup>rd</sup> / 4 <sup>th</sup> effects
Temperature (°C)	104 / 92 / 80 / 68
Pressure (atm)	1.15 / 0.739 / 0.459 / 0.225
Heat transfer coefficients (kW/m <sup>2</sup> °C)	2.56 / 1.86 / 1.395 / 0.815
<b>Crystallizer</b>	
Temperature (°C)	25
Residence time (h)	12
Ethanol concentration (%wt)	70%
<b>Mannose solubility data in 80% ethanol <sup>15</sup></b>	
<b>T (°C)</b>	<b>C (g/L)</b>
5.05	183.75
15.05	198.84
25.05	210.56

<sup>a</sup> based on separation yields reported for galacto- and fructo-oligosaccharides<sup>16,17</sup>

Table S6. Operational parameters for the MOS purification section (S-600)

<b>Equipment and parameters</b>	<b>Values</b>
<b>Multi-effect Evaporator</b>	1 <sup>st</sup> / 2 <sup>nd</sup> / 3 <sup>rd</sup> / 4 <sup>th</sup> effects
Temperature (°C)	110 / 97 / 81 / 52
Pressure (atm)	1.409 / 0.893 / 0.482 / 0.1
Heat transfer coefficients (kW/m <sup>2</sup> °C)	2.56 / 1.86 / 1.395 / 0.815
<b>Activated carbon (AC) columns</b>	
HMF and furfural removal efficiency	95% <sup>18,19</sup>
Sugars loss	5% <sup>18,19</sup>
Water wash volume (BV)	1
Ethanol volume (BV)	1
<b>Sizing parameters</b>	
Adsorption capacity (mg HMF/g AC)	300 <sup>20</sup>
AC density (kg/m <sup>3</sup> )	400 <sup>21</sup>
Equipment overdesign factor	2
Bed to column height ratio	0.5
H/D ratio	3

Table S7. Operational parameters for the combustion section (S-700)

<b>Equipment and parameters</b>	<b>Values</b>
<b>Boiler</b>	
Outlet temperature (°C)	1050
Excess air for combustion (%)	10%
<b>Steam turbine</b>	
Adiabatic efficiency (%)	90%
<b>Alternative 1: single pressure Rankine cycle</b>	
Inlet temperature (°C)	560
Inlet pressure (atm)	27.34
Outlet pressure (atm)	0.095
<b>Alternative 2: dual pressure Rankine cycle</b>	
Live steam temperature (°C)	540
Live steam pressure (atm)	70.00
Exhaust steam pressure (atm)	19.74
Outlet pressure (atm)	0.095

Table S8. Operational parameters for the cold utilities section (S-800)

Equipment and parameters	Values
<b>Cooling tower</b>	
Air humidity	80%
Air temperature (°C)	28
Inlet water temperature (°C)	43
Cooling water temperature (°C)	35
<b>Propane Chiller</b>	
Inlet water temperature (°C)	25
Chilled water temperature (°C)	15
Propane pressure (atm)	6.22
Compressor discharge pressure (atm)	16.2
Compressor isentropic efficiency	80%

## 2. Statistical models for dilute-oxalic acid hydrolysis of açaí seeds

The second order models obtained for mannose yield ( $Y_{1/0}$ ), mannan conversion ( $\chi_1$ ), and mass loss ( $\delta_1$ ) are given in Equations 1–3.

$$\hat{Y}_{1/0} = 0.5106 + 0.2370 c_1 - 0.0481 c_1^2 + 0.0645 c_2 + 0.0442 c_3 - 0.0520 c_1 c_3 \quad (1)$$

$$\hat{\chi}_1 = 0.5359 + 0.2964 c_1 + 0.0597 c_1^2 + 0.0755 c_2 + 0.0453 c_3 \quad (2)$$

$$\hat{\delta}_1 = 0.4343 + 0.2002 c_1 + 0.0299 c_1^2 + 0.0429 c_2 + 0.0361 c_3 \quad (3)$$

where  $c_1$ ,  $c_2$ , and  $c_3$  represent the dimensionless coded values of temperature, acid concentration, and time, respectively. Coded values are obtained from their original variables by subtracting the central value and dividing the result by the spacing between the central and high levels of each factor ( $c_1=(x_1-150)/20$ ,  $c_2=(x_2-4.0)1.5$ , and  $c_3=(x_3-40)/15$ ).

Table S9 shows the analyses of variance (ANOVA) of the fitted models, which were significant with p-value < 0.0001 and showed excellent correlation with the experimental data ( $R^2 > 90\%$ ). The p-value for lack of fit of the mannose yield model does not affect the model validity as it can be considered a result of a very small deviation in the central points, which led to a low value of pure error and thus a significant p-value in the F-test.

Table S9. Analysis of variance of the adjusted models for mannose yield, mannan conversion, and mass loss for oxalic acid hydrolysis of açaí seeds

Variation source	Sum of squares	Degrees of freedom	Mean square	F <sub>calc</sub>	p-value
<b>Mannose yield (<math>Y_{1/0}</math>)</b>					
Regression	8869.1	5	1773.8	20.3	0.00003
Residuals	961.0	11	87.4		
Lack of Fit	957.9	9	106.4	68.8	0.01441
Pure Error	3.1	2	1.5		
Total	9830.1	16			
R <sup>2</sup>	90.22%				
<b>Mannan conversion (<math>\chi_1</math>)</b>					
Regression	12018.3	4	3004.6	101.6	3.80E-09
Residuals	354.9	12	29.6		
Lack of Fit	336.7	10	33.7	3.7	0.23130
Pure Error	18.2	2	9.1		
Total	12373.2	16			
R <sup>2</sup>	97.13%				
<b>Mass loss (<math>\delta_1</math>)</b>					
Regression	5430.4	4	1357.6	120.8	1.39E-09
Residuals	134.8	12	11.2		
Lack of Fit	130.0	10	13.0	5.4	0.165888
Pure Error	4.8	2	2.4		
Total	5565.3	16			
R <sup>2</sup>	97.58%				

### 3. Additional data

Figure S1 presents the experimental pH values of oxalic acid solutions employed for açaí seeds hydrolysis, which were used to calculate the CSF of each hydrolysis condition. The final pH values of açaí seeds' hydrolysates are also shown, revealing that pH variations throughout the hydrolysis reactions were not significant. In addition, theoretical pH values of oxalic acid and sulfuric acid solutions are included for comparison. Theoretical pH values were calculated from the acids' dissociation constants:  $k_{a1} = 5.370 \cdot 10^{-2}$  and  $k_{a2} = 5.248 \cdot 10^{-5}$  for oxalic acid, corresponding to  $pK_{a1} = 1.27$  and  $pK_{a2} = 4.28$  at 25 °C;<sup>22</sup> and  $k_{a2} = 1.02 \cdot 10^{-2}$  for sulfuric acid,<sup>23</sup> corresponding to  $pK_{a2} = 1.99$ . The differences between theoretical and experimental values for oxalic acid solutions may be attributed to low measurement accuracy in low pH ranges.

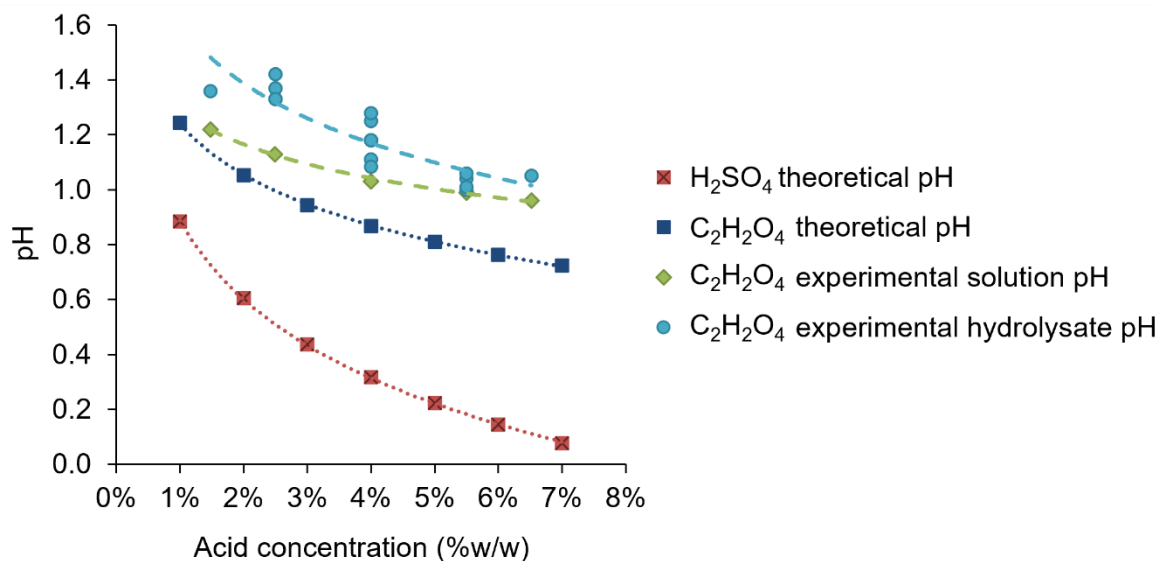


Figure S1. Theoretical and experimental pH values of oxalic acid solutions at different concentrations and experimental pH values of açaí seeds hydrolysates after dilute oxalic acid hydrolysis. Theoretical pH values for sulfuric acid solutions are also shown for comparison.

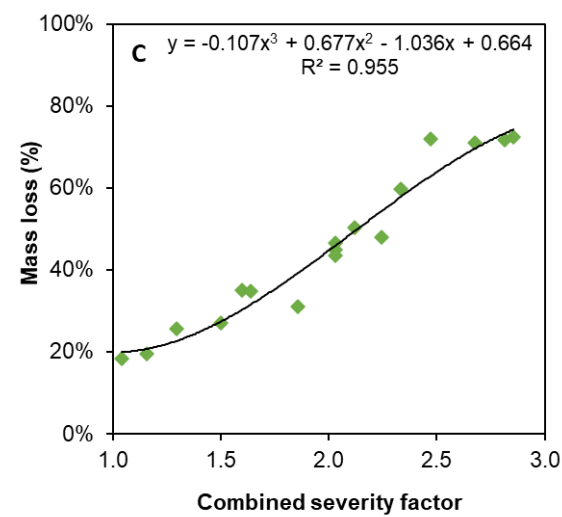
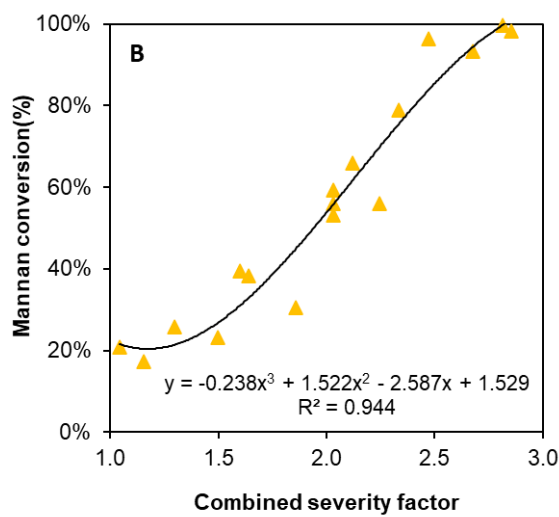
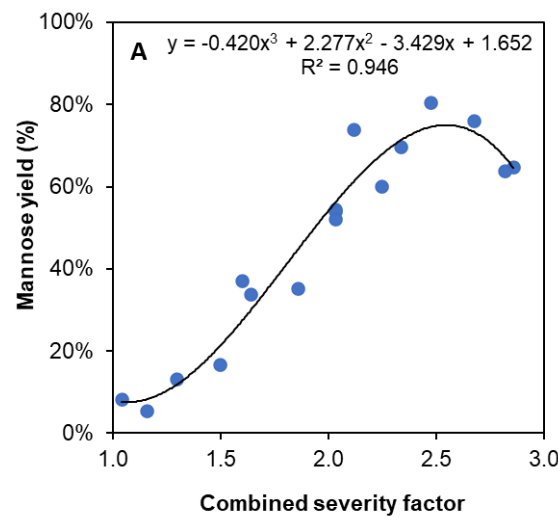


Figure S2. Correlations between the combined severity factor and response variables of dilute-oxalic acid hydrolysis of açaí seeds optimization: a) mannose yield, b) mannan conversion, c) mass loss.

## References

- 1 M. K. D. Rambo, F. L. Schmidt and M. M. C. Ferreira, *Talanta*, 2015, **144**, 696–703.
- 2 A. F. Monteiro, I. S. Miguez, J. P. R. B. Silva and A. S. da Silva, *Sci. Rep.*, 2019, **9**, 1–12.
- 3 M. Luczynski, MSc thesis, Universidade Federal do Pará, 2008.
- 4 L. Bufalino, A. A. Guimarães, B. M. D. S. E. Silva, R. L. F. de Souza, I. C. N. A. de Melo, D. N. P. S. de Oliveira and P. F. Trugilho, *J. Renew. Sustain. Energy*, 2018, **10**, 053102.
- 5 D. A. R. de Castro, Universidade Federal do Pará, 2019.
- 6 G. Saravacos and A. E. Kostaropoulos, *Handbook of Food Processing Equipment*, Springer International Publishing AG Switzerland, Athens, Greece, Second Edi., 2016.
- 7 K. L. Kenney, K. G. Cafferty, J. J. Jacobson, I. J. Bonner, G. L. Gresham, J. R. Hess, L. P. Orvard, W. A. Smith, D. N. Thompson, V. S. Thompson, J. S. Tumuluru and N. Yancey, *Feedstock Supply System Design and Economics for Conversion of Lignocellulosic Biomass to Hydrocarbon Fuels. Conversion Pathway: Biological Conversion of Sugars to Hydrocarbons*, Idaho Falls, Idaho, 2013.
- 8 D. Humbird, R. Davis, L. Tao, C. Kinchin, D. Hsu, A. Aden, P. Schoen, J. Lukas, B. Olthof, M. Worley, D. Sexton and D. Dudgeon, *Process Design and Economics for Biochemical Conversion of Lignocellulosic Biomass to Ethanol: Dilute-Acid Pretreatment and Enzymatic Hydrolysis of Corn Stover*, Golden, CO, 2011.
- 9 Y. Xie, D. Phelps, C. H. Lee, M. Sedlak, N. Ho and N. H. L. Wang, *Ind. Eng. Chem. Res.*, 2005, **44**, 6816–6823.
- 10 W. A. Farone, J. E. Cuzens, US Pat., 5820687A, 1998.
- 11 G. Lodi, G. Storti, L. A. Pellegrini and M. Morbidelli, *Ind. Eng. Chem. Res.*, 2017, **56**, 1621–1632.
- 12 R. D. Hester, G. E. Farina, S. Nangueri, US Pat., 5407580A, 1995.
- 13 H. A. Ruiz, M. Conrad, S.-N. Sun, A. Sanchez, G. J. M. Rocha, A. Romaní, E. Castro, A. Torres, R. M. Rodríguez-Jasso, L. P. Andrade, I. Smirnova, R.-C. Sun and A. S. Meyer, *Bioresour. Technol.*, 2020, **299**, 122685.
- 14 A. R. Oroskar, N. S. Sudharsan, P. A. Oroskar, O. M. Kulkarni, US Pat., 9163050B2, 2015.
- 15 X. Gong, C. Wang, L. Zhang and H. Qu, *J. Chem. Eng. Data*, 2012, **57**, 3264–3269.
- 16 I. Mueller, A. Seidel-Morgenstern and C. Hamel, *Sep. Purif. Technol.*, 2021, **271**, 1–11.
- 17 K. Vaňková and M. Polakovič, *Chem. Eng. Technol.*, 2012, **35**, 161–168.
- 18 Z. Lin, J. Wang, V. Nikolakis and M. Ierapetritou, *Comput. Chem. Eng.*, 2017, **102**, 258–267.
- 19 T. Sainio, I. Turku and J. Heinonen, *Bioresour. Technol.*, 2011, **102**, 6048–6057.
- 20 P. Vinke and H. van Bekkum, *Starch - Stärke*, 1992, **44**, 90–96.
- 21 R. H. Perry and D. W. Green, *Perry's Chemical Engineers' Handbook*, 1997.
- 22 H. Kayser, F. Rodríguez-Ropero, W. Leitner, M. Fioroni and P. D. de María, *RSC Adv.*,

2013, **3**, 9273–9278.

- 23 H. Sippola and P. Taskinen, *J. Chem. Eng. Data*, 2014, **59**, 2389–2407.